Aerosol and Air Quality Research, 15: 1627–1639, 2015

ISSN: 1680-8584 print / 2071-1409 online
doi: 10.4209/aaqr.2014.12.0329

Comparison of Emissivity, Transmittance, and Reflectance Infrared Spectra of Polycyclic Aromatic Hydrocarbons with those of Atmospheric Particulates (PM_1)

Dayana M. Agudelo-Castañeda[1], Elba Calesso Teixeira[1,2*], Ismael Luís Schneider[1], Silvia Beatriz Alves Rolim[1], Naira Balzaretti[3], Gabriel Silva e Silva[3]

[1] *Programa de Pós-Graduação em Sensoriamento Remoto, Universidade Federal do Rio Grande do Sul, Porto Alegre, RS, Brazil*
[2] *Fundação Estadual de Proteção Ambiental Henrique Luís Roessler, Porto Alegre, RS, Brazil*
[3] *Instituto de Física, Universidade Federal do Rio Grande do Sul, Porto Alegre, RS, Brazil*

ABSTRACT

Polycyclic Aromatic Hydrocarbons (PAHs) are a group of various complex organic compounds composed of carbon and hydrogen, and two or more condensed benzene rings. They are released into the atmosphere by the incomplete combustion or pyrolysis of organic matter. Some of the major sources of PAHs are burning of coal, wood, oil or gas, vehicle engines exhaust, and open burning. PAHs are of great concern to human health mainly because of their known carcinogenic and mutagenic properties. Consequently, it is very important to study atmospheric PAHs, especially those associated with ultrafine particles. This study aims to identify the spectral features of PAHs in samples of particulate matter < 1 μm (PM_1) using infrared spectrometry. Emissivity and transmittance spectra of PAHs were obtained by infrared spectroscopy. PAHs standards spectra contributed to effectively identify PAHs in PM_1 samples. Emissivity and transmittance spectra in the range of 680–900 cm^{-1} exhibited the largest number of bands due to C–C out-of-plane angular deformations and C–H out-of-plane angular deformations. Bands of medium intensity in 2900–3050 cm^{-1} region were also observed due to C–H stretching typical of aromatic compounds, although with lower intensity. This study compared the emissivity and transmittance spectra acquired using two different infrared spectrometers in order to identify PAHs in samples of atmospheric particulate matter and analyzed the capability and advantages of each of the infrared spectrometers. In addition, it was confirmed that the PAHs under study can be distinguished by their infrared spectral fingerprints.

Keywords: FTIR; Emissivity; Transmittance; Particulate matter; PAH.

INTRODUCTION

Particulate matter (PM) is considered as one of the major pollutants that affect the health of humans, especially for the fine and ultrafine fraction, which can adsorb greater concentrations of toxic compounds, e.g., polycyclic aromatic hydrocarbons-PAHs (Silva *et al.*, 2009; Ribeiro *et al.*, 2010; Kronbauer *et al.*, 2013; Dias *et al.*, 2014; Garcia *et al.*, 2014; Pérez *et al.*, 2014). Atmospheric aerosols contribute to adverse health and environmental effects, visibility degradation, and radiative forcing (Jacobson and Hansson, 2000). In order to understand and control the impacts of atmospheric aerosols, it is important to determine the physical and chemical properties of aerosols (Coury and Dillner, 2009). Various studies have pointed to vehicular emissions as the main source of fine and ultrafine particles in urban environments (Harrison *et al.*, 1999; Shi and Harrison, 1999; Shi *et al.*, 1999). PAHs are a group of several complex organic compounds consisting of carbon and hydrogen, and two or more condensed benzene rings and represent one of the most stable families of organic compounds known (Ravindra *et al.*, 2008). PAHs may exist in large number of different structures, depending on the complexity and the number of isomers. PAHs represent a great public health concern (Panther *et al.*, 1999) and they constitute a group of widespread pollutants of great environmental interest. PAHs and their metabolites are among the most toxic, carcinogenic, and mutagenic atmospheric contaminants known (Nagabalasubramanian and Periandy, 2010).

The key sources of atmospheric emission of PAHs are incomplete combustion or pyrolysis of organic matter (Li *et al.*, 2005). Vehicular exhausts and combustion of coal, wood, or oil are the major contributors of PAHs in the atmosphere. In an urban environment, vehicular exhausts, especially those from diesel engines, are the main sources of PAHs (Tsapakins *et al.*, 2002; Guo, 2003; Fang *et al.*,

* Corresponding author.
Tel.: +55 51 3288-9408
E-mail address: gerpro.pesquisa@fepam.rs.gov.br

2004; Manoli *et al.*, 2004; Ravindra *et al.*, 2006; Ströher *et al.*, 2007). PAHs released into the air may react with gases present in the atmosphere that might transform them into products that are probably more dangerous than they are in their native forms (i.e., nitrated PAHs). Moreover, organic compounds may enhance or inhibit the water-uptake characteristics of the fine particles (Blando *et al.*, 2001).

In general, planar PAHs are more stable, less reactive, and biologically less toxic (Cerqueira *et al.*, 2011; Silva *et al.*, 2011; Cerqueira *et al.*, 2012; Oliveira *et al.*, 2012a, b; Quispe *et al.*, 2012; Silva *et al.*, 2012; Arenas-Lago *et al.*, 2013; Oliveira *et al.*, 2013; Ribeiro *et al.*, 2013; Cutruneo *et al.*, 2014; Saikia *et al.*, 2014). Whereas, substitution of methyl or other groups into the ring system of PAH can result in molecular distortion from planarity that sometimes translates into more reactivity and carcinogenicity. The chemistry of PAHs allows for an extreme diversity in their molecular structure. Also, the arrangement of aromatic rings and the possibility of numerous substitutions and side-chains allow for numerous permutations in the structure of PAHs (Izawa *et al.*, 2014). The effects of changes in the molecular structure of PAHs and their composition on solid-state reflectance spectra (ultraviolet, visible, and near-infrared) were investigated using pure PAHs. Researchers also studied the fate of PAHs in the environment (transformation, degradation) and their effect on the health (toxicity) that depends of environmental factors (He *et al.*, 2009).

Many studies have explored the analysis of PAHs in PM using gas chromatography associated with mass spectrometry (GC/MS) (Dallarosa *et al.*, 2005a, b; Teixeira *et al.*, 2012; Agudelo-Castañeda and Teixeira, 2014). Some of the disadvantages associated with GC/MS analysis are the requirement of a relatively large amount of aerosol mass, extraction, complex derivatization procedures for detecting compounds of varying polarity, and it is not possible to detect large molecules (Yu *et al.*, 1998). Spectroscopic techniques has some advantages over chromatographic techniques in aerosol particle analysis. Advantages includes the ability to perform chemical fingerprinting; the ability to detect compounds in smaller concentrations without extraction or derivatization (nondestructive method) and the possibility of using the instrumentation in the sampling site. Thus the losses may be diminished of the samples during their transportation, cooling and storage; also, smaller sample sizes may be used with no requirement for sample preparation (Allen and Palen, 1989; Allen *et al.*, 1994; Marshall *et al.*, 1994; Coury and Dillner, 2008; Navarta *et al.*, 2008). In addition, in spectroscopic techniques, several samples can be selected in order to perform GC/MS quantitative analysis at a later stage, thus reducing economic costs.

Moreover, Fourier transform infrared spectroscopy (FTIR) can be used to identify a compound or investigate the chemical composition of a sample using its vibrational spectrum, which is considered as one of its most characteristic physico-chemical properties, particularly in organic compounds. The vibrational modes depend on the type of the internal structure of the constituents, the size of the ionic radius, and the bonding forces and ionic impurities contained in the matter (Meneses, 2001). The total energy contained in a material is composed of the components associated with the electronic, vibrational, rotational, and translational energy. The infrared spectrum covers only the spectral region corresponding to vibrational and rotational modes giving intrinsic information on the chemical and structural composition of the material. Infrared spectroscopy has been widely used to determine the composition of submicron particles (Maria *et al.*, 2003; Liu *et al.*, 2009; Russell *et al.*, 2011), although these works do not study PAHs.

In the present study, the Fourier transformed infrared emissivity and transmittance spectra of particulate matter of size < 1 μm (PM_1) and that of solid standards of PAHs were compared to study the efficiency of these techniques in the identification of PAHs in PM_1 samples collected on filters without prior treatment. This study gains significance since these PM_1 samples are hazardous than larger particles because they can enter the respiratory tract (Slezakova *et al.*, 2007). Moreover, these particles possess larger specific area and hence can adsorb high concentrations of toxic, mutagenic, and/or carcinogenic compounds.

MATERIALS AND METHODS

Sampling of Atmospheric Particulate Matter

PM_1 sampling was performed in an automatic sequential particle sampler model PM162M from Environment S.A. at a volumetric flow rate of 1.0 m^3/h. PM_1 samples were collected using Zefluor™ membrane PTFE (polytetrafluorethylene) filters of 47 mm diameter, specifically designed for organic sampling (Peltonen and Kuljukka, 1995). The equipment for collection of particulate matter < 1 μm (PM_1) was installed at the following geographic coordinates (UTM) 29°49′06″S/51°09′34″W (Sapucaia do Sul) and 29°55′50″S/51°10′56″W (Canoas). Sapucaia do Sul and Canoas are located at south Brazil, in Rio Grande do Sul State. Canoas is under a strong vehicular influence, daily traffic congestions, Canoas air base and industries (oil refinery) upstream of the prevailing winds that have a medium influence in this sampling site. Sapucaia do Sul site has a greater vehicular influence vehicle: light and heavy fleet, traffic congestions and slow speeds. This site also has low industrial influence (oil refinery, steel mills that do not use coke, Canoas Air Force Base) upstream of prevailing winds. Sampling was carried out at a constant flow rate of 1 m^3/h for 72 and 12 hours for the determination of emissivity (FTIR) and transmittance spectra. These sampling times were found to be appropriate for a good resolution of bands corresponding to organic species. Several studies show that PTFE filters are more adapted for FTIR tests and have lower absorption bands (overlapping peaks) in infrared analyses than nucleopore or quartz filters (Ghauch *et al.*, 2006).

Instruments

Emissivity spectra were obtained using a Model 102F portable FTIR spectrometer by Design and Prototypes at *Centro Estadual de Pesquisa em Sensoriamento Remoto e Meteorologia* (CEPSRM) (State Research Center for Remote Sensing and Meteorology) of the Federal University of Rio

Grande do Sul (UFRGS). The FTIR spectrometer consists of an optical/electronic module, Michelson interferometer, and infrared detectors. It is equipped with two detectors, an InSb (Indio-antimony) and a MCT (Mercury-cadmium-tellurium) detector covering 3330–2000 cm^{-1} and 2000–700 cm^{-1} spectral ranges, respectively, cooled by liquid nitrogen (Salisbury, 1998), and two blackbodies that can be set at different temperatures in the range of 5–60°C during the instrument calibration. The spectra were analyzed in the range of 1660–700 cm^{-1}, with a spectral resolution of 4 cm^{-1} and spectral accuracy of ± 1 cm^{-1}. The 1660–3330 cm^{-1} range was not analyzed due to low signal/noise ratio of the equipment in this range (Korb *et al.*, 1996). Furthermore, within this range (1660–3330 cm^{-1}) transmittance is low due to the presence of absorption bands of methane, CO_2, and water vapor (Korb *et al.*, 1996). The data were obtained from an average of 100 scans, i.e., 100 co-added interferograms. The measurements were performed at a distance of less than 50 cm to minimize atmospheric attenuation (Korb *et al.*, 1996) using a foreoptic of diameter 2.54 cm to ensure that the field of view (FOV) was smaller than the sample with a diameter of 47 mm. In addition, all emissivity measurements were performed under conditions of clear sky without clouds with low to moderate relative humidity (< 60%).

Transmittance spectra were obtained by a BOMEM MB-series FTIR-Hartmann & Braun Michelson spectrometer equipped with DTGS detector at the Institute of Physics of Federal University of Rio Grande do Sul (UFRGS). Fifty scans of transmittance spectra with a resolution of 4 cm^{-1} were performed in the range of 400–4000 cm^{-1} to obtain an appropriate signal/noise. Transmittance spectra were collected from each sample of PM_1 and are presented in arbitrary units (a.u.), using a background spectrum of blank filter without sample.

Calibration and Operation of the FTIR Spectrometer

Emission and responsiveness of the instrument were calibrated with blackbodies under controlled temperatures (Salisbury, 1998). Calibration consisted of measuring the radiation of two blackbodies at two known temperatures and the background emission of the instrument was deducted. In addition, downwelling radiance calibration was also performed. Downwelling radiance of the hemisphere above the target is measured by a reflector located at the target, a gold plate with emissivity of ε = 0.040 in the spectral range. More details on the radiometric calibration of the instrument can be found in the studies by Hook and Kahle (1996) and Korb *et al.* (1996).

The measured radiance actually consists of the sum of various radiances entering the equipment, and for the conditions used in the present study the relation between the radiances can be written as (Salvaggio and Miller, 2001):

$$L_s(\lambda) = \varepsilon_s(\lambda)B(\lambda,T_S) + [1-\varepsilon_S(\lambda)]L_{DWR}(\lambda) \quad (1)$$

where, $L_S(\lambda)$ is the total spectral radiance entering the sensor; $B(\lambda,T_S)$ is the radiance of a blackbody at the sample temperature (T_S); $(1 - \varepsilon_s)$ is the sample reflectance; and L_{DWR} is the downwelling radiance.

Sample emissivity can be determined using Eq. (2), where the radiance measured must be divided by the Planck function of blackbody radiance at the sample temperature (T_S), which is unknown.

$$\varepsilon_s(\lambda) = \frac{L_s(\lambda) - L_{DWR}(\lambda)}{B(\lambda,T_s) - L_{DWR}(\lambda)} \quad (2)$$

where,

$\varepsilon_s(\lambda)$: emissivity of the sample surface as a function of the wavelength

$L_s(\lambda)$: calibrated radiance of the sample

$L_{DWR}(\lambda)$: calibrated radiance of the incident radiance

$B(\lambda,T_s)$: Planck function at the sample temperature

Sample temperature was defined as described by Johnson *et al.* (1998) and Ribeiro da Luz and Crowley (2007). Initially, temperature measured by an infrared digital thermometer Minipa MT-350 with accuracy of ± 2°C was selected. Fig. 1 shows an example of emissivity spectra obtained as a function of the diverse temperatures chosen. This spectrometer calculates the spectra in μm, which was converted to frequency (cm^{-1}) in order to compare the results with other studies. Water bands at 8.18, 8.24, and 12.58 μm show the residual characteristics of the downwelling radiance (Ribeiro da Luz, 2005), as observed in Fig. 1 indicated by arrows. If the temperature chosen is higher than the actual temperature of the sample (overestimated temperature), the residual characteristics of the downwelling radiance will point downwards. If the temperature chosen is lower than that of the sample, the residual characteristics will point upwards (underestimated temperature), similarly to the downwelling radiance (Horton *et al.*, 1998). The correct emissivity spectrum was obtained through a trial-and-error process, i.e., in which the residual characteristics of the downwelling radiance were minimized. The spectrum obtained at 32°C did not show the residual characteristics of downwelling radiance indicating the appropriate temperature. The configuration geometry of the emissivity measurements was as follows: distance of < 50 cm between the sensor and the sample; sample size of 47 mm diameter; optical angle of 90°.

Preparation and Analysis of the PAHs Solid Standards

For transmittance spectra, the PAH solid standards of fluoranthene, pyrene, benzo [α]pyrene and benzo[α]anthracene with 99% purity were obtained from Sigma Aldrich and were prepared in solid KBr pellets to obtain transmittance spectra. For emissivity spectra, PAHs solid standards were used as received and placed in 50 mm diameter dishes. In both cases, PM_1 samples were analysed directly without any preparation, and the molecular vibrations of the two classes of spectra were identified using sources in the literature (Semmler *et al.*, 1991; Carrasco Flores *et al.*, 2005; Onchoke *et al.*, 2006; Onchoke and Parks 2011).

Using FTIR D&P spectrometer, experimental emissivity spectra of solid standards of PAHs fluoranthene and pyrene were obtained. The signature molecular vibrations from the spectra were identified by comparison with the spectral database (Semmler *et al.*, 1991; Allen *et al.*, 1994; Carrasco Flores *et al.*, 2005; Reff *et al.*, 2005; Onchoke *et al.*, 2006;

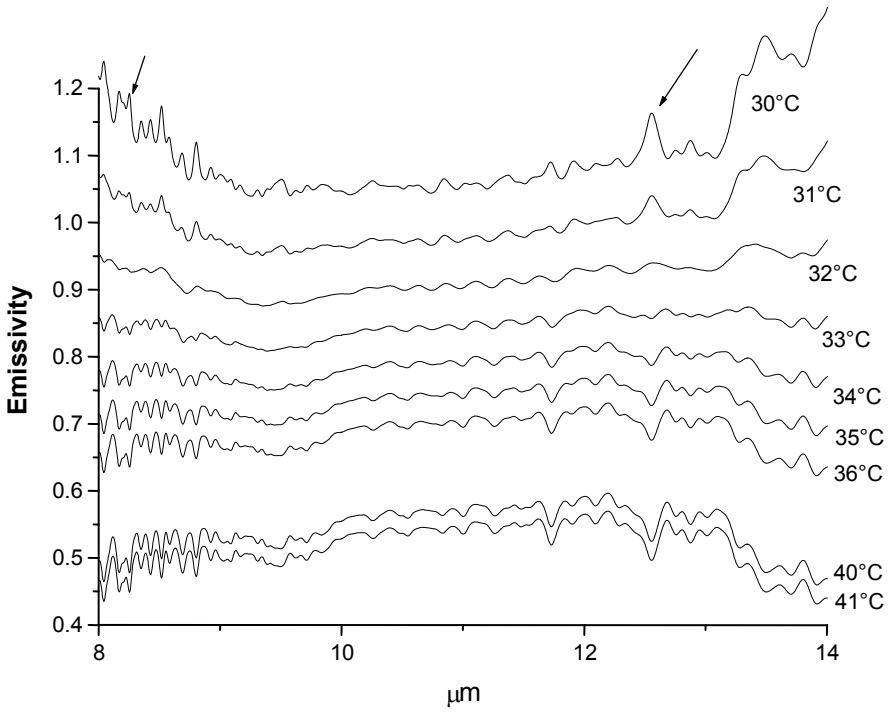

Fig. 1. Emissivity spectra obtained for a sample temperature range of 30°C to 41°C. Water bands at 8.18, 8.24, and 12.58 μm show the residual characteristics of the downwelling radiance indicated by arrows.

Tsai and Kuo, 2006; Reff *et al.*, 2007; Hopey *et al.*, 2008; Polidori *et al.*, 2008; Onchoke and Parks, 2011).

Experimental transmittance spectra of solid standards of the PAHs viz. fluoranthene, pyrene, benzo[*a*]pyrene, benzo[*a*]anthracene were obtained using the BOMEM MB-series FTIR-Hartmann & Braun Michelson spectrometer. The molecular vibrations of transmittance spectra were identified from the literature (Semmler *et al.*, 1991; Carrasco Flores *et al.*, 2005; Onchoke *et al.*, 2006; Onchoke and Parks, 2011).

RESULTS

Spectra of PAHs Solid Standards

Emissivity

Figs. 2(a) and 2(b) show the emissivity spectrum of fluoranthene and pyrene, respectively. The emissivity of fluoranthene spectrum (Fig. 2(a)) was observed to have peaks of higher intensity than that of pyrene spectrum (Fig. 2(b)). Table 1 presents the representative peaks observed in the experimental emissivity spectra of fluoranthene and pyrene. The absorption bands corresponding to CO_2 and atmospheric water vapor in the range of 700 cm^{-1} and 1646 cm^{-1} were excluded from Table 1 (Jellison and Miller, 2004). The vibrations from C–C out-of-plane angular deformation and C–H out-of-plane (Table 1) were identified in the range of 700–850 cm^{-1} for both the standards. Previous studies (Semmler *et al.*, 1991) have shown that at least one band is present in the range of 600–900 cm^{-1} in the spectra of PAHs.

Intense and moderate intensity bands were observed in the spectra of fluoranthene at 830 cm^{-1} and 734 cm^{-1} corresponding to C–C out-of-plane angular deformation and C–H out-of-plane angular deformation (Hudgins and Sandford, 1998b; Semmler *et al.*, 1991). In the case of pyrene, peaks at 849 cm^{-1} and 734 cm^{-1} were assigned to C–C out-of-plane angular deformation and C–H out-of-plane angular deformation (Hudgins and Sandford, 1998a; Semmler *et al.*, 1991). The spectral range of 1000–1300 cm^{-1} contains various peaks of low intensity due to C–H in-plane aromatic angular deformations (Table 1), except for 1100 cm^{-1}, where the peaks relating to C–C stretch and C–H in-plane angular deformation can be observed (Kubicki, 2001). In the range from 1350–1570 cm^{-1}, peaks of high intensity were observed for the fluoranthene spectrum, whereas they appear with low intensity ones in the pyrene spectrum. In the fluoranthene spectrum (Table 1), the peaks were mostly due to the presence of five rings of cyclopentadienyl (Hudgins and Sandford, 1998a). For pyrene (Table 1), the peaks were observed mainly in the range of 1313–1323 cm^{-1}, resulting from the C–H in-plane angular deformation. The peaks in the range 1358–1488 cm^{-1} appear due to C–C stretch and C–H in-plane angular deformation only in the fluoranthene spectra.

Transmittance

Figs. 3(a)–3(c), and d present the transmittance spectra of solid standards of pyrene, benzo[*a*]anthracene, benzo[*a*]pyrene, and fluoranthene recorded on KBr pellets, respectively. The designation of the peaks identified in the transmittance spectra of fluoranthene, pyrene, benzo[*a*]pyrene, and benzo[*a*]anthracene are presented in Table 1. The peaks at ≈2300 cm^{-1} representing the CO_2 absorption bands were excluded (Jellison and Miller, 2004). Similar to the emissivity spectra observed in the

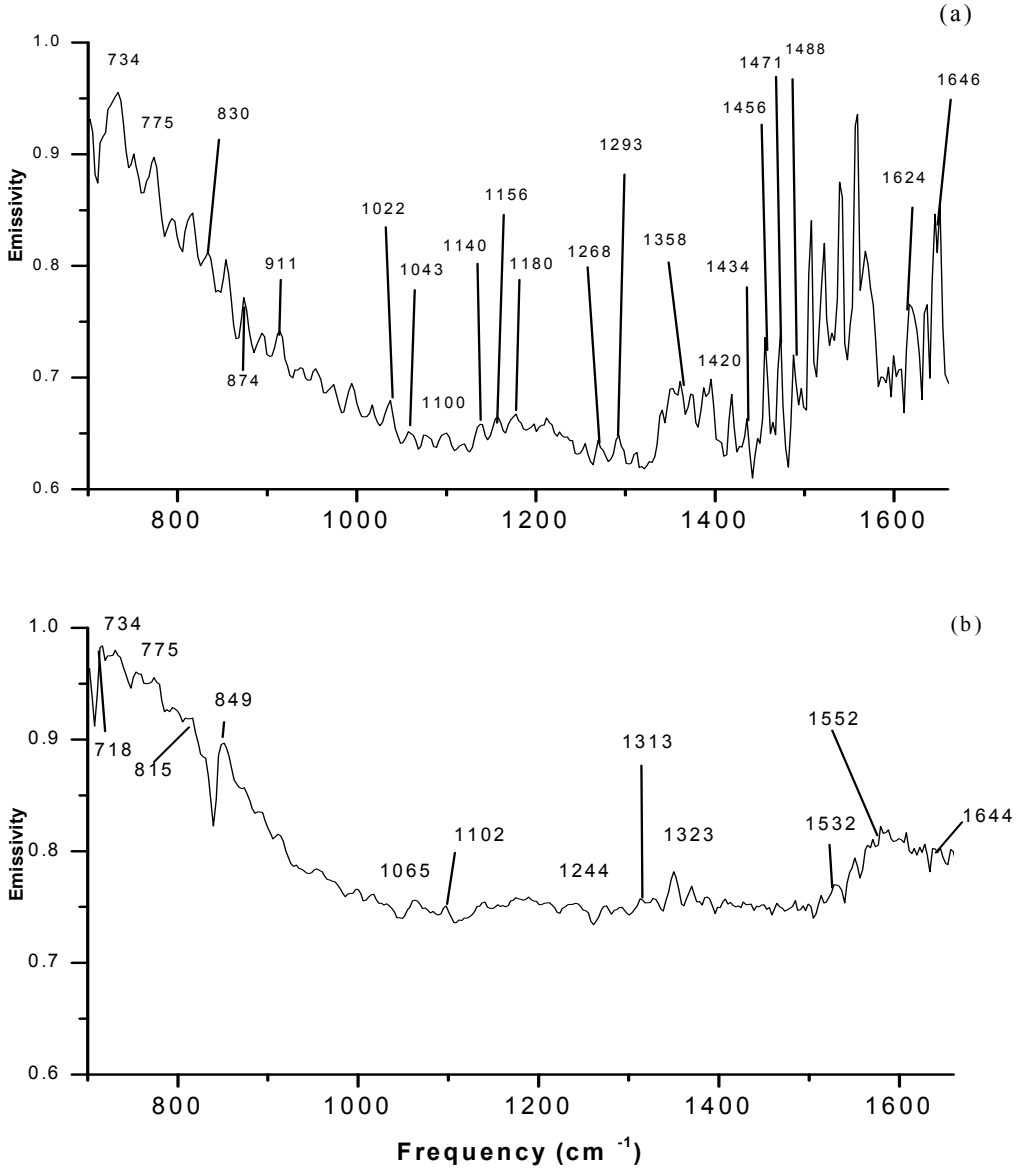

Fig. 2. Emissivity spectra of Fluoranthene (a) and Pyrene (b) solid standards recorded in 47-mm dishes.

Table 1. Designation of features identified in the experimental emissivity spectra of fluoranthene and pyrene in the 700–1660 cm^{-1} spectral range and in the transmittance spectra of Fluoranthene, Pyrene, Benzo[a]Pyrene and Benzo[a]Anthracene in the 400–4000 cm^{-1} spectral range. Unit: cm^{-1}.

Fluoranthene		Pyrene		Benzo[a] Pyrene	Benzo[a] Anthracene	Vibrational
Emissivity	Transmittance	Emissivity	Transmittance	Transmittance	Transmittance	assignments
	426				422	γ (CC) + γ(CH)
				455		γ (CC) + γ(CH)
					471	δ(CC) + δ(CH)
	482					δ(CC) + δ(CH)
			496			δ(CC)
					511	γ(CH)
				534		γ(CH)
			540			γ(CC) + γ(CH)
	617					τ(CCCC) + ν(CH)
				635		γ(CC) + γ(CH)
					648	γ(CH)
				689	689	γ (CC)

Table 1. *(continued).*

Fluoranthene		Pyrene		Benzo[a] Pyrene	Benzo[a] Anthracene	Vibrational
Emissivity	Transmittance	Emissivity	Transmittance	Transmittance	Transmittance	assignments
		710	708			γ (CC) + γ(CH)
		718				γ (CC) + γ(CH)
734		734				γ (CC) + γ(CH)
	746		748		748	γ(CH)
				762		γ(CH)
775	775	775				γ (CC) + γ(CH)
					783	γ(CH)
	826	815		822	812	γ(CH)
830			839	835		γ(CH)
		849				γ(CH)
874				874		γ(CH)
					885	γ(CH)
911	910		912			γ(CH)
	939					γ(CH)
				945		γ(CH)
					953	γ(CH)
			962			γ(CH)
	970					γ(CH)
					1009	δ(CH)
1022						ν(CC) + δ(CH)
				1034	1038	δ(CH)
1043						δ(CH)
		1065				δ(CH)
1100		1102	1095		1097	*ν*(CC) + δ(CH)
				1121		*ν*(CC) + δ(CH)
1140	1134		1136			δ(CH)
1156	1159			1163		δ(CH)
				1176		δ(CH)
1180	1182		1184			δ(CH)
	1215					*ν*(CC) + δ(CH)
		1244	1240	1244	1238	*ν*(CC) + δ(CH)
1268				1269		*ν*(CC) + δ(CH)
1293	1290					δ(CH)
		1313	1312	1312		*ν*(CC)+δ(CH)
		1323				δCH
1358						ν(CC) + δ(CH)
				1408		*ν*(CC)
					1414	*ν*(CC) + δ(CH)
1420	1425					ν(CC) + δ(CH)
1434			1433			ν(CC) + δ(CH)
	1439					δ(CH)
1456	1452			1458		*ν*(CC) + δ(CH)
1471						ν(CC) + δ(CH)
1488	1485					*ν*(CC) + δ(CH)
					1499	*ν*(CC) + δ(CH)
		1532				ν(CC) + δ(CH)
		1552				ν(CC) + δ(CH)
			1593	1595		*ν*(CC)
1624						ν(CC) + δ(CH)
		1644				ν(CC) + δ(CH)
1646						ν(CC)
	3037/3049		3028/3043	3030/3074	3030/3047	$\nu(CH)_{(aromatic)}$

ν = Stretch; δ = In plane; γ = Out of plane.

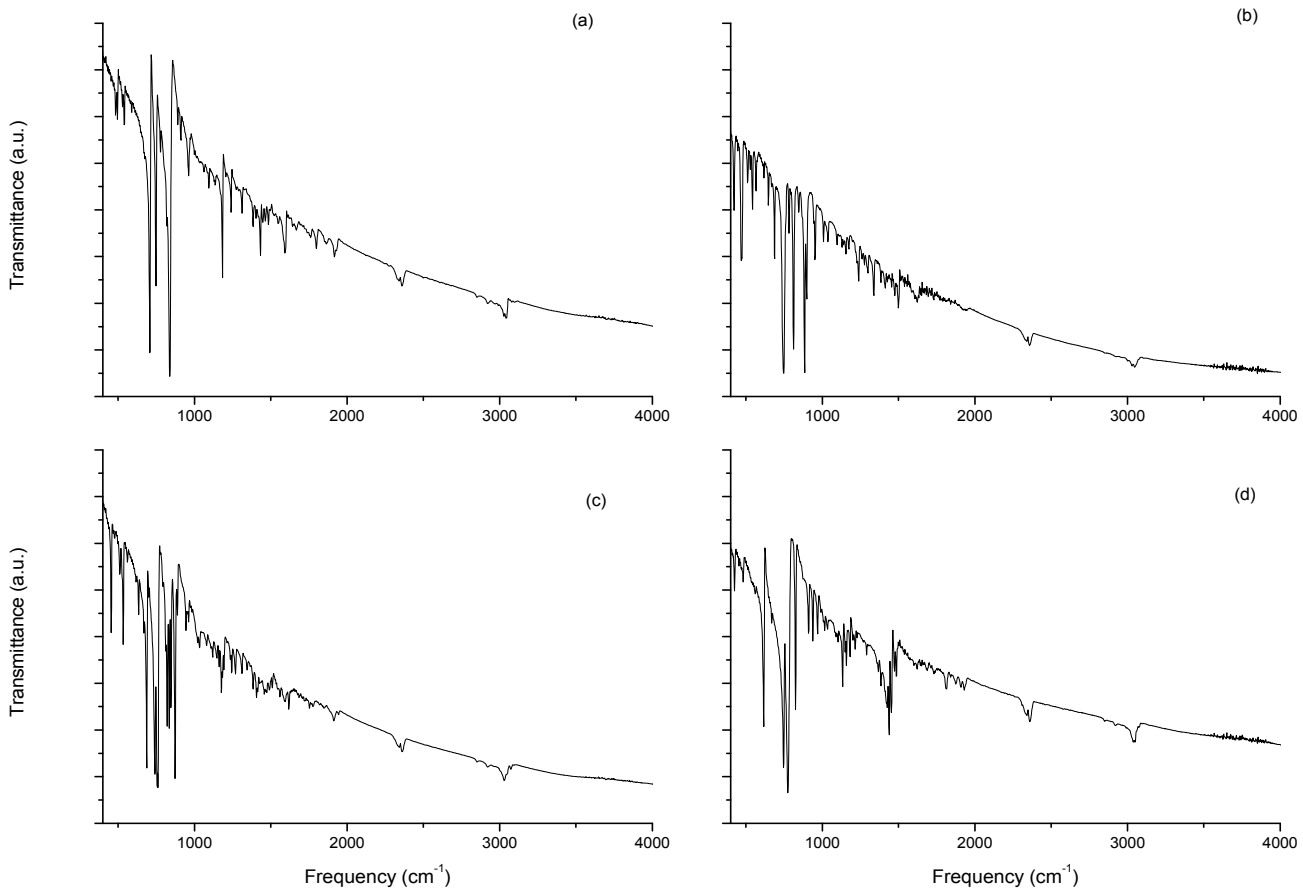

Fig. 3. Transmittance spectra of Pyrene (a), Benzo[a]anthracene (b) Benzo[a]pyrene (c), Fluoranthene (d) solid standards recorded on KBr pellets.

PAHs transmittance spectra, strong bands in the 600–900 cm^{-1} range due to C–C out-of-plane angular deformations and C–H out-of-plane angular deformations, and bands of medium and low intensity in 1000–1500 cm^{-1} spectral range were observed. Bands in the 900–2000 cm^{-1} spectral range were also observed, however with lower intensity, except for the CO_2 band at ≈2300 cm^{-1}. In 3000–3100 cm^{-1} spectral range, bands, typical of aromatic compounds, due to C–H stretch were observed.

Spectra of Samples of Atmospheric Particulate Matter (PM_1)

Emissivity

Figs. 4(a) and 4(b) shows the emissivity spectra of samples (PM_1) collected in Canoas and Sapucaia do Sul, respectively. In the emissivity spectra (Fig. 4), peaks can be observed in the range of 730–850 cm^{-1} resulting from C–C out-of-plane angular deformation and C–H out-of-plane angular deformation. Also, peaks in the range of 1350–1500 cm^{-1} resulting from C–C stretch vibrations and C–H in-plane angular deformation can be observed. The emissivity spectra of PM_1 samples (Fig. 4) displayed different peaks occurring in the 1620–1650 cm^{-1} spectral range. An array of compounds absorb radiation in this region, including -OH present in water, alcohols, and carboxylic acids, and the carbonyl stretch (C = O) such as amides that are more conjugated than aldehydes, ketones and acids (Reff *et al.*, 2005). For example, the vibrational mode v_2 of liquid water occurs at 1640 cm^{-1}. Thus, these bands overlap and hinder the identification of organic compounds. Moreover, the emissivity spectra exhibit a peak at ~1100 cm^{-1} which corresponds to the carbon-fluorine bond (C–F); consequently, bands at this frequency may overlap and hence, cannot be identified unambiguously (Ghauch *et al.*, 2006). With reference to the identification of PAHs, a peak may be observed at ≈830 cm^{-1} in both the spectra (Figs. 4(a) and 4(b)), indicating a C–H out-of-plane angular deformation, possibly associated with an aromatic group (Wang *et al.*, 2007). Other peaks can also be observed in the range of 600–900 cm^{-1}, a spectral region where vibrations of C–C and C–H out-of-plane angular deformation can occur, including that of the PAHs (Semmler *et al.*, 1991). Various authors have shown that the spectral region in the range of 700–900 cm^{-1} is most characteristic and distinctive for the identification of PAHs molecules (Langhoff, 1996); and that in PAHs spectra, at least one band is found in 680–900 cm^{-1} spectral range (Semmler *et al.*, 1991). Moreover, several others have defined 770–900 cm^{-1} spectral range as typical of PAHs, that corresponds to the C–H out-of-plane angular deformation (Szczepanski and Vala, 1993; Hudgins *et al.*, 1994; Langhoff, 1996). Consequently, the bands observed in the emissivity spectra of PM_1 samples (Figs. 4(a) and 4(b)) at ≈732 cm^{-1},

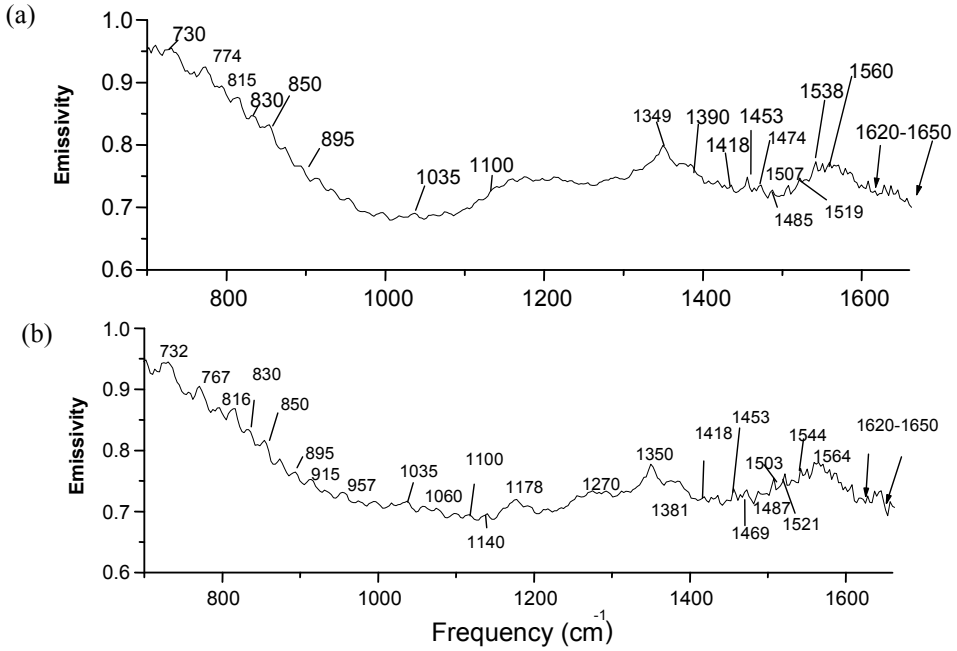

Fig. 4. Emissivity spectra of PM_1 sample collected in Canoas (a), May 2–5, 2012, and in Sapucaia do Sul (b), Jan 22–25, 2012.

≈767 cm^{-1}, ≈774 cm^{-1}, ≈815 cm^{-1}, ≈830 cm^{-1}, and ≈850 cm^{-1} are possibly related to molecular vibrations of PAHs. The band at ≈732 cm^{-1} may be due to four neighboring C–H units; the bands at ≈767 cm^{-1}/≈774 cm^{-1} due to three neighboring C–H units; and those at ≈815 cm^{-1}/≈830 cm^{-1}/≈850 cm^{-1} to two neighboring C–H units (Semmler *et al.*, 1991). Bands were also observed in 1000–1500 cm^{-1} spectral range due to vibrations of C–C stretch and C–H in-plane angular deformation. PAHs spectra also presented at least one band in 3000–3100 cm^{-1} spectral range due to C–H aromatic stretch.

Transmittance

Figs. 5(a)–5(c) shows the transmittance spectra of PM_1 samples collected at Sapucaia do Sul on May 11, 2013 (Fig. 5(a)), at Canoas on May 27, 2013 (Fig. 5(b)) and May 4, 2013 (Fig. 5(c)). Canoas transmittance spectrum collected on May 27, 2013 (Fig. 5(b)) showed less strong peaks than the others did (Figs. 5(a) and 5(c)). Probably, the particulate matter concentration in this sample and, consequently, of organic compounds and PAHs, was lower than that in the other samples. All the spectra (Figs. 5(a)–5(c)) showed different peaks in 600–900 cm^{-1} spectral range, corresponding to the vibrations of the aromatic rings, which were also identified in the spectra of PAHs standards. Some peaks were also centered in 1000–1500 cm^{-1} spectral range, corresponding to the C = C of aromatics, in addition to the C–H out-of-plane angular deformation. Nevertheless, in the transmittance spectra, the peaks in 1250–1300 cm^{-1} range correspond to the carbon-fluorine (C–F) bond. In this region, a high intensity peak was observed due to the influence of the filter (PTFE), and hence, bands of the compounds at this frequency cannot be identified unambiguously.

As discussed in Section "Spectra of PAHs solid standards", the aromatic organic compounds have low intensity peaks in 3000–3100 cm^{-1} range resulting from the vibrations from C–H of aromatic groups. Consequently, the bands observed in the PM_1 samples showed low intensity in this spectral region, probably due to low organic compound concentrations (few nanograms per cubic meter), especially PAHs (Allen *et al.*, 1994; Teixeira *et al.*, 2013). For example, the bands in 3000–3100 cm^{-1} spectral range were observed only in Figs. 5(a) and 5(c), but not in Fig. 5(b).

Fig. 5(a) shows the transmittance spectrum of the particulate matter in the sample collected in Sapucaia do Sul on May 11, 2013. The transmittance spectrum (Fig. 5(a)), in 600–900 cm^{-1} spectral range, showed a peak at 634 cm^{-1} that was identified in the spectrum of Benzo[*a*]pyrene (Table 1). Although, at this frequency (634 cm^{-1}) molecular vibrations from sulfite ions (SO_3^{2-}) present in the particulate matter can be observed (Tsai and Kuo, 2006). Peaks were observed at 715, 783, and 856 cm^{-1}, corresponding to 5, 3, and 2 C–H neighboring units (connected) in the PAHs, respectively (Semmler *et al.*, 1991). At 1000–1500 cm^{-1} spectral range, the transmittance spectrum presented peaks at 1049, 1157, 1255, and 1467 cm^{-1}. At 1049 cm^{-1} and 783 cm^{-1} frequencies, overlapping may occur due to SiO_4^{-4} ion, which also generates frequencies in this region, typical of silicate ions (Tsai and Kuo, 2006). Some of these bands were identified in the fluoranthene spectrum and benzo[*a*]pyrene spectrum (Table 1), due to C–H out-of-plane angular deformations or C–C stretch. A peak was also identified at 3041 cm^{-1} due to aromatic C–H stretch, observed in the spectra of diverse PAHs, including pyrene. Peaks at 2920 cm^{-1} and 1722 cm^{-1} suggest the presence of aliphatic and carbonyl, respectively.

Fig. 5(b) shows the transmittance spectrum of the particulate matter contained in the sample collected in Canoas on May 27, 2013. The spectrum shows peaks at

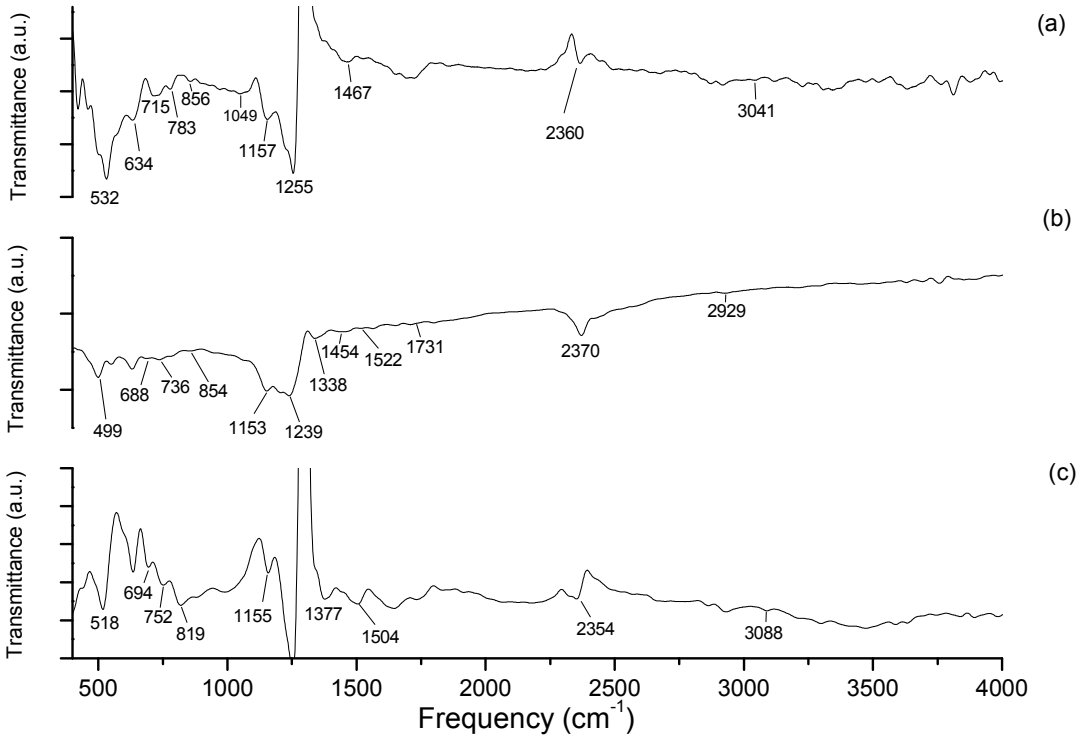

Fig. 5. Transmittance spectra of PM_1 samples collected in (a) Sapucaia do Sul, May 11, 2013, (b) Canoas, May 27, 2013 and (c) Canoas, May 4, 2013.

688 cm^{-1}, 736 cm^{-1}, and 854 cm^{-1} due to C–H out-of-plane angular deformations of 5, 4, and 2 CH neighboring units, respectively. Nonetheless, at 688 cm^{-1} molecular vibrations arising from sulfite ions (SO_3^{2-}) may occur (Tsai and Kuo, 2006). Bands were also identified at 1153, 1239, and 1338 cm^{-1} due to C–H in-plane angular deformations, and at 1454 and 1522 cm^{-1} due to C–C stretch and C–H in-plane angular deformations, respectively. As explained above, bands in the 3000–3100 cm^{-1} spectral range were not found. Vibrations from carbonyl and aliphatic groups were observed in bands 1731 and 2929 cm^{-1}, respectively.

Fig. 5(c) shows the transmittance spectrum of the particulate matter in the sample collected in Canoas on May 4, 2013. The transmittance spectrum (Fig. 5(c)) shows peaks at 694, 752, and 819 cm^{-1}. In this case, the corresponding bands were observed in the benzo[*a*]pyrene, benzo[*a*]anthracene, fluoranthene, and pyrene standards (Table 1). Also, at 694 cm^{-1}, molecular vibrations from sulfite ions (SO_3^{2-}) may occur (Tsai and Kuo, 2006). The transmittance spectrum presented peaks at 1377 cm^{-1} and 1504 cm^{-1} (1000-1500 cm^{-1} spectral range). A peak in the 3000–3100 cm^{-1} spectral range, at 3088 cm^{-1}, was observed. This spectral region presents molecular vibrations arising from C–C in-plane angular deformations and C–H out-of-plane aromatic.

DISCUSSION

Firstly, it may be observed that the emissivity/transmittance spectra of the PAH solid standards (Figs. 2 and 3) showed clear and stronger bands when compared with those of PM_1 samples. This is probable because the intensity and width of the bands depend on composition and density (Kubicki, 2001). Broader bands in the PM_1 sample spectra (Figs. 4 and 5) can be attributed as a result of the interaction between PAH and the surface (Dabestani and Ivanov, 1999); and also to the fact that the particulate matter was collected in an heterogeneous media (e.g., adsorbed onto a filter). In addition, the forms and intensities depend on the relative masses and bonding forces (Hamilton, 2010). Secondly, when comparing emissivity and transmittance spectra obtained by different spectrometers, it might be observed that the peak intensities are different. The intensity of peaks in the transmittance spectra is higher than it is in emissivity spectra at lower frequencies, e.g., < 1000 cm^{-1}. Consequently, several clear peaks were observed in 600–900 cm^{-1} range, a spectral region with molecular vibrations typical of PAHs. Thirdly, emissivity spectra (both for PAHs standards and PM_1 samples) identified more peaks in the 1000–1500 cm^{-1} range than do transmittance spectra, which only showed few peaks. Finally, emissivity spectra showed more peaks in the 600–900 cm^{-1} in PM_1 samples (Fig. 4) than do transmittance spectra (Fig. 5). However, the transmittance spectra technique has the advantage of a larger spectral range (400–4000 cm^{-1}), including 3000–3100 cm^{-1} region. This region contains the frequencies of the C–H stretch m(C–H), in which some frequencies that are essential to the identification of PAHs may occur.

Concisely, samples of atmospheric particulate matter can be characterized by diverse methods using infrared spectroscopy, either in laboratory or *in situ*. The FTIR spectrometer (used to obtain emissivity spectra) is advantageous since it can be carried to the field, thus

reducing errors caused by transportation or cooling of the samples, whereas measurements of transmittance spectra using conventional FTIR spectrometer must be performed in laboratory, which increases the probability of errors. Nevertheless, transmittance technique has some advantages over emissivity techniques in that it has; (i) a larger spectral range; (ii) no interferences in the measurements taken *in situ* due to the presence of atmospheric gases. Thus, this study contributes to the knowledge on both the techniques with regards to the identification of PAHs in atmospheric particulate matter collected on filters. The choice of an appropriate technique depends on the goals of measurement. Each of the methods discussed in this study offers unique experimental resources and requires further studies that would analyze the merits and demerits on the quantification of compounds in the samples.

CONCLUSIONS

We conclude that the measurements of both emissivity and transmittance spectra using infrared spectroscopy are useful methods for the analysis of atmospheric particulate matter. Moreover, the spectra of PAHs standards contributed more effectively towards the identification of PAHs in the atmospheric particulate matter collected on filters. These measurements contributed heavily to the successful comparison of two methods in the identification of PAHs. This study confirms that PAHs may be differentiated by their infrared spectral fingerprints using the two methods described here albeit they are poorly studied. We expect that infrared spectroscopy becomes a technique not only to study functional groups, organic or inorganic composition of particle matter, but also PAHs. This study strives to contribute to the knowledge and understanding of these techniques for the analyses of PAHs, since these pollutants are of great health concern; especially, benzo[a]pyrene, classified as carcinogenic to humans according to the International Agency for Research on Cancer (IARC, 2010). Also, the IARC report, Air Pollution and Cancer (IARC, 2013) emphasizes the importance of studying these pollutants using different techniques such that they may be implemented anywhere in the world, including the undeveloped countries.

ACKNOWLEDGMENTS

To FAPERGS and CNPq for the financial support.

REFERENCES

Agudelo-Castañeda, D.M. and Teixeira, E.C. (2014). Seasonal Changes, Identification and Source Apportionment of PAH in $PM_{1.0}$. *Atmos. Environ.* 96: 186–200.

Allen, D.T. and Palen, E. (1989). Recent Advances in Aerosol Analysis by Infrared Spectroscopy. *J. Aerosol Sci.* 20: 441–455.

Allen, D.T., Palen, E.J., Haimov, M.I., Hering, S.V. and Young, J.R. (1994). Aerosol Science and Technology Fourier Transform Infrared Spectroscopy of Aerosol Collected in a Low Pressure Impactor (LPI/FTIR): Method Development and Field Calibration. *Aerosol Sci. Technol.* 4: 37–41.

Arenas-Lago, D., Veja, F.A., Silva, L.S. and Andrade, L. (2013). Soil Interaction and Fractionation of Added Cadmium in Some Galician Soils. *Microchem. J.* 110: 681–690.

Blando, J.D., Porcja, R.J. and Turpin, B.J. (2001). Issues in the Quantitation of Functional Groups by FTIR Spectroscopic Analysis of Impactor-Collected Aerosol Samples. *Aerosol Sci. Technol.* 35: 899–908.

Carrasco Flores, E., Campos Vallette, M.M., Clavijo, R.E.C., Leyton, P., Díaz, F. and Koch, R. (2005). SERS Spectrum and DFT Calculations of 6-nitrochrysene on Silver Islands. *Vib. Spectrosc.* 37: 153–160.

Cerqueira, B., Vega, F.A., Serra, C., Silva, L.F.O. and Andrade, M.L. (2011). Time of Flight Secondary Ion Mass Spectrometry and High-resolution Transmission Electron Microscopy/Energy Dispersive Spectroscopy: A Preliminary Study of the Distribution of Cu^{2+} and Cu^{2+}/Pb^{2+} on a Bt Horizon Surfaces. *J. Hazard. Mater.* 195: 422–431.

Cerqueira, B., Vega, F.A., Silva, L.F.O. and Andrade, L. (2012). Effects of Vegetation on Chemical and Mineralogical Characteristics of Soils Developed on a Decantation Bank from a Copper Mine. *Sci. Total Environ.* 421–422: 220–229.

Coury, C. and Dillner, A.M. (2008). A Method to quantify Organic Functional Groups and Inorganic Compounds in Ambient Aerosols Using Attenuated Total Reflectance FTIR Spectroscopy and Multivariate Chemometric Techniques. *Atmos. Environ.* 42: 5923–5932.

Coury, C. and Dillner, A.M. (2009). ATR-FTIR Characterization of Organic Functional Groups and Inorganic Ions in Ambient Aerosols at a Rural Site. *Atmos. Environ.* 43: 940–948.

Cutruneo, C.M.N.L., Oliveira, M.L.S., Ward, C.R., Hower, J.C., de Brum, I.A.S., Sampaio, C.H., Kautzmann, R.M., Taffarel, S.R., Teixeira, E.C. and Silva, L.F.O. A. (2014). Mineralogical and Geochemical Study of Three Brazilian Coal Cleaning Rejects: Demonstration of Electron Beam Applications. *Int. J. Coal Geol.* 130: 33–52.

Dabestani, R. and Ivanov, N.I. (1999). A compilation of Physival, Spectroscopic and Photophysical Properties of Polycyclic Aromatic Hydrocarbons. *Photochem. Photobiol.* 70: 10–34.

Dallarosa, J.B., Teixeira, E.C., Pires, M. and Fachel, J. (2005a). Study of the Profile of Polycyclic Aromatic Hydrocarbons in Atmospheric Particles (PM_{10}) Using Multivariate Methods. *Atmos. Environ.* 39: 6587–6596.

Dallarosa, J., Monego, J., Teixeira, E.C., Stefens, J. and Wiegand, F. (2005b). Polycyclic Aromatic Hydrocarbons in Atmospheric Particles in the Metropolitan Area of Porto Alegre, Brazil. *Atmos. Environ.* 39: 1609–1625.

Di Filippo, P., Riccardi, C., Pomata, D. and Buiarelli, F. (2010). Concentrations of PAHs, and Nitro- and Methyl-Derivatives Associated with a Size-segregated Urban Aerosol. *Atmos. Environ.* 44: 2742–2749.

Dias, C.L., Oliveira, M.L.S., Hower, J.C., Taffarel, S.R.,

Kautzmann, R.M., Silva, L.F.O. (2014). Nanominerals and Ultrafine Particles from Coal Fires from Santa Catarina, South Brazil. *Int. J. Coal Geol.* 122: 50–60.

Fang, G.C., Chang, C.N., Wu, Y.S., Fu, P.P.C., Yang, I.L. and Chen, M.H. (2004). Characterization, Identification of Ambient Air and Road Dust Polycyclic Aromatic Hydrocarbons in Central Taiwan, Taichung. *Sci. Total Environ.* 327: 135–146.

Garcia, K.O., Teixeira, E.C., Agudelo-Castaneda, D.M., Braga, M., Alabarse, P.G., Wiegand, F., Kautzmann, R.M. and Silva, L.F.O. (2014). Assessment of Nitro-polycyclic Aromatic Hydrocarbons in PM_1 near an Area of Heavy-duty Traffic. *Sci. Total Environ.* 479–480: 57–65.

Ghauch, A., Deveau, P.A., Jacob, V. and Baussand, P. (2006). Use of FTIR Spectroscopy Coupled with ATR for the Determination of Atmospheric Compounds. *Talanta* 68: 1294–1302.

Guo, H. (2003). Particle-associated Polycyclic Aromatic Hydrocarbons in Urban Air of Hong Kong. *Atmos. Environ.* 37: 5307–5317.

Hamilton, V.E. (2010). Thermal Infrared (Vibrational) Spectroscopy of Mg – Fe Olivines: A Review and Applications to Determining the Composition of Planetary Surfaces. *Chem. Erde* 70: 7–33.

Harrison, R.M., Jones, M. and Collins, G. (1999). Measurements of the Physical Properties of Particles in the Urban Atmosphere. *Atmos. Environ.* 33: 309–321.

He, Y.Y., Wang, X.C., Jin, P.K., Zhao, B. and Fan, X. (2009). Complexation of Anthracene with Folic Acid Studied by FTIR and UV Spectroscopies. *Spectrochim. Acta, Part A* 72: 876–879.

Hook, S.J. and Kahle, A.B. (1996). The Micro Fourier Transform Intefferometer (μFTIR) A New Field Spectrometer for Acquisition of Infrared Data of Natural Surfaces. *Remote Sens. Environ.* 56: 172–181.

Hopey, J., Fuller, K., Krishnaswamy, V., Bowdle, D. and Newchurch, M.J. (2008). Fourier Transform Infrared Spectroscopy of Size-segregated Aerosol Deposits on Foil Substrates. *Appl. Opt.* 47: 2266–2274.

Horton, K.A., Johnson, J.R. and Lucey, P.G. (1998). Infrared Measurements of Pristine and Disturbed Soils 2. Environmental Effects and Field Data Reduction. *Remote Sens. Environ.* 64: 47–52.

Hudgins, D.M., Sandford, S. and Allamandola, L.J. (1994). Infrared Spectroscopy of Polycyclic Aromatic Hydrocarbon Cations. 1. Matrix-isolated Naphthalene and Perdeuterated Naphthalene. *J. Phys. Chem.* 98: 4243–4253.

Hudgins, D.M. and Sandford, S.A. (1998a). Infrared Spectroscopy of Matrix Isolated Polycyclic Aromatic Hydrocarbons. 1. PAHs Containing Two to Four Rings. *J. Phys. Chem.* 5639: 329–343.

Hudgins, D.M. and Sandford, S.A. (1998b). Infrared Spectroscopy of Matrix Isolated Polycyclic Aromatic Hydrocarbons. 3. Fluoranthene and the Benzofluoranthenes. *J. Phys. Chem.* 5639: 353–360.

IARC, International Agency for Research on Cancer (2010). Monographs, Supplement, http://monographs.iarc.fr/ENG/Classification/, Last Accessed: December of 2013).

IARC, International Agency for Research on Cancer (2013). In Air Pollution and Cancer, Vol 161, Straif, K., Cohen, A., Samet, J. (Eds.), IARC Scientific Publications.

Izawa, M.R.M., Applin, D.M., Norman, L. and Cloutis, E.A. (2014). Reflectance Spectroscopy (350–2500nm) of Solid-state Polycyclic Aromatic Hydrocarbons (PAHs). *Icarus* 237: 159–181.

Jacobson, M.C. and Hansson, H. (2000). Organic Atmospheric Aerosol, Review and State of Science. *Rev. Geophys.* 38: 267–294.

Jellison, G.P. and Miller, D.P. (2004). Plume Structure and Dynamics from Thermocouple and Spectrometer Measurements. *Proc. SPIE* 5425: 232–243.

Johnson, J.R., Lucey, P.G., Horton, K.A. and Winter, E.M. (1998). Infrared Measurements of Pristine and Disturbed Soils 1. Spectral Contrast Differences between Field and Laboratory Data. *Remote Sens. Environ.* 46: 34–46.

Korb, A.R., Dybwad, P., Wadsworth, W. and Salisbury, J. W. (1996). Portable Fourier Transform Infrared Spectroradiometer for Field Measurements of Radiance and Emissivity. *App. Opt.* 35: 1679–1692.

Kronbauer, M.A.; Izquierdo, M., Dai, S., Waanders, F.B., Wagner, N.J., Mastalerz, M., Hower, J.C., Oliveira, M.L.S., Taffarel, S.R., Bizani, D. and Silva, L.F.O. (2013). Geochemistry of Ultra-fine and Nano-compounds in Coal Gasification Ashes: A Synoptic View. *Sci. Total Environ*. 456–457: 95–103, 2013.

Kubicki, J.D. (2001). Interpretation of Vibrational Spectra Using Molecular Orbital Theory Calculations. *Rev. Mineral. Geochem.* 42: 459–483.

Langhoff, S.R. (1996). Theoretical Infrared Spectra for Polycyclic Aromatic Hydrocarbon Neutrals, Cations, and Anions. *J. Phys. Chem.* 100: 2819–2841.

Li, M., McDow, S.R., Tollerud, D.J. and Mazureka, M.A. (2005). Seasonal Abundance of Organic Molecular Markers in Urban Particulate Matter from Philadelphia, PA. *Atmos. Environ.* 40: 2260–2273.

Liu, S., Takahama, S., Russell, L.M., Gilardoni, S. and Baumgardner, D. (2009). Oxygenated Organic Functional Groups and Their Sources in Single and Submicron Organic Particles in MILAGRO 2006 Campaign. *Atmos. Chem. Phys.* 9: 6949–6863.

Manoli, E., Kouras, A. and Samara, C. (2004). Profile Analysis of Ambient and Source Emitted Particle-bound Polycyclic Aromatic Hydrocarbons from Three Sites in Northern Greece. *Chemosphere* 56: 867–878.

Maria, S.F., Russell, L.M, Turpin, B.J., Porcja, R.J., Campos, T.L., Weber, R.J. and Huebert, B.J. (2003). Source Signatures of Carbon Monoxide and Organic Functional Groups in Asian Pacific Regional Aerosol Characterization Experiment (ACE-Asia) Submicron Aerosol Types. *J. Geophys. Res.-Atmos.* 108: 8637.

Marshall, T.L., Chaffin, C.T., Hammaker, R.M. and Fateley, W.G. (1994). An Introduction to Open-path FT-IR. Atmospheric Monitoring. *Environ. Sci. Technol.* 28: 224A–232A.

Meneses, P.R. and Netto, J.S.M. (2001). *Sensoriamento Remoto: Reflectância dos Alvos Naturais.* Editora da

Universidade de Brasília, Brasília.

Nagabalasubramanian, P.B. and Periandy, S. (2010). FTIR and FT Raman, Molecular Geometry, Vibrational Assignments, Ab Initio and Density Functional Theory Calculations for 1,5-methylnaphthalene. *Spectrochim. Acta, Part A* 77: 1099–1107.

Navarta, M.D.F., Ojeda, C.B. and Rojas, F.S. (2008). Aplicación de la Espectroscopia del Infrarrojo Medio en Química Analítica de Procesos. *Bol. Soc. Quim. Mex.* 2: 93–103.

Oliveira, M.L.S., Ward, C.R., French, D., Hower, J.C., Querol, X. and Silva, L.F.O. (2012a). Mineralogy and Leaching Characteristics of Beneficiated Coal Products from Santa Catarina, Brazil. *Int. J. Coal Geol.* 94: 314–325.

Oliveira, M.L.S., Ward, C.R., Izquierdo, M., Sampaio, C.H., de Brum, I.A.S., Kautzmann, R.M., Sabedot, S., Querol, X. and Silva, L.F.O. (2012b). Chemical Composition and Minerals in Pyrite Ash of an Abandoned Sulphuric Acid Production Plant. *Sci. Total Environ*. 430: 34–47.

Oliveira, M.L.S., Ward, C.R., Sampaio, C.H., Querol, X., Cutruneo, C.M.N.L., Taffarel, Silvio, R. and Silva, L.F.O. (2013). Partitioning of Mineralogical and Inorganic Geochemical Components of Coals from Santa Catarina, Brazil, by Industrial Beneficiation Processes. *Int. J. Coal Geol.* 116: 75–92.

Onchoke, K.K. and Parks, M. (2001). Experimental and Theoretical Study of Vibrational Spectra of 3-nitrofluoranthene. *J. Mol. Struct.* 999: 22–28.

Onchoke, K.K., Hadad, C.M. and Dutta, P.K. (2006). Structure and Vibrational Spectra of Mononitrated Benzo[a]pyrenes. *J. Phys. Chem.* 110: 76–84.

Panther, B.C., Hooper, M.A. and Tapper, N.J. (1999). A Comparison of Air Particulate Matter and Associated Polycyclic Aromatic Hydrocarbons in Some Tropical and Temperate Urban Environments. *Atmos. Environ.* 33: 4087–4099.

Peltonen, K. and Kuljukka, T. (1995). Air Sampling and Analysis of Polycyclic Aromatic Hydrocarbons. *J. Chromatogr. A* 710: 93–108.

Pérez, F., Llorca, M., Kock-Schulmeyer, M. Krbi, B., Oliveira, L.S., Da Boit Martinello, K., Al-Dhabi, N.A., Anti, I., Farré, M. and Barcelò, D. (2014). Assessment of Perfluoroalkyl Substances in Food Items at Global Scale. *Environ. Res.* 135: 181–189.

Polidori, A., Turpin, B.J., Davidson, C.I., Rodenburg, L. and Maimone, F. (2008). Organic $PM_{2.5}$: Fractionation by Polarity, FTIR Spectroscopy, and OM/OC Ratio for the Pittsburgh Aerosol. *Aerosol Sci. Technol.* 42: 233–246.

Quispe, D., Pérez-López, R., Silva, L.F.O. and Nieto, J.M. (2012). Changes in Mobility of Hazardous Elements during Coal Combustion in Santa Catarina Power Plant (Brazil). *Fuel* 94: 495–503.

Ravindra, K., Bencs, L., Wauters, E., De Hoog, J., Deutsch, F., Roekens, E., Bleux, N., Berghmans, P. and Van Grieken, R. (2006). Seasonal and Site-specific Variation in Vapour and Aerosol Phase PAHs over Flanders (Belgium) and Their Relation with Anthropogenic Activities. *Atmos. Environ.* 40: 771–785.

Ravindra, K., Sokhi, R. and Vangrieken, R. (2008). Atmospheric Polycyclic Aromatic Hydrocarbons: Source Attribution, Emission Factors and Regulation. *Atmos. Environ.* 42: 2895–2921.

Reff, A., Turpin, B.J., Porcja, R.J., Giovennetti, R., Cui, W., Weisel, C.P., Zhang, J., Kwon, J., Alimokhtari, S., Morandi, M., Stock, T., Maberti, S., Colome, S., Winer, A., Shendell, D., Jones, J. and Farrar, C. (2005). Functional Group Characterization of Indoor, Outdoor, and Personal PM: Results from RIOPA. *Indoor Air* 15: 53–61.

Reff, A., Turpin, B.J., Offenberg, J.H., Weisel, C.P., Zhang, J., Morandi, M., Stock, T., Colome, S. and Winer, A. (2007). A Functional Group Characterization of Organic $PM_{2.5}$ Exposure: Results from the RIOPA Study. *Atmos. Environ.* 41: 4585–4598.

Ribeiro da Luz, B. (2005). *Propriedades Espectrais das Plantas no Infravermelho Termal (2.5-14 μm): da Química ao Dossel.* – São Paulo. PhD Thesis. São Paulo University. 188pp.

Ribeiro da Luz, B. and Crowley, J.K. (2007). Spectral Reflectance and Emissivity Features of Broad Leaf Plants: Prospects for Remote Sensing in the Thermal Infrared (8.0–14.0 μm). *Remote Sens. Environ.* 109: 393–405.

Ribeiro, J., Flores, D., Ward, C.R. and Silva, LF.O. (2010). Identification of Nanominerals and Nanoparticles in Burning Coal Waste Piles from Portugal. *Sci. Total Environ*. 408: 6032–6041.

Ribeiro, J., Taffarel, S.R., Sampaio, C.H., Flores, D., Silva, L.F.O. (2013). Mineral Speciation and Fate of Some Hazardous Contaminants in Coal Waste Pile from Anthracite Mining in Portugal. *Int. J. Coal Geol.* 109–110: 15–23.

Russell, L.M., Bahadura, R. and Ziemann, P.J. (2011). Identifying Organic Aerosol Sources by Comparing Functional Group Composition in Chamber and Atmospheric Particles. *Proc. Nat. Acad. Sci. U.S.A.* 108: 3516–3521.

Saikia, B.K., Ward, C.R., Oliveira, M.L.S., Hower, J.C., Braga, M. and Silva, L.F. (2014). Geochemistry and Nano-mineralogy of Two Medium-sulfur Northeast Indian Coals. *Int. J. Coal Geol.* 122: 26–34.

Salisbury, J.W. (1998). Spectral Measurements Field Guide. Published by the Defense Technology Information Center as Report No. ADA362372, Earth Satellite Corporation.

Salvaggio, C. and Miller, C.J. (2001). Methodologies and Protocols for the Collection of Midwave and Longwave Infrared Emissivity Spectra Using a Portable Field Spectrometer. *Proc. SPIE* 4381, doi: 10.1117/12.437046.

Semmler, J., Yang, P.W. and Crawford, G.E. (1991). Gas Chromatography/Fourier Transform Infrared Studies of Gas-phase Polynuclear Aromatic Hydrocarbons. *Vib. Spectrosc.* 2: 189–203.

Shi, J.P. and Harrison, R.M. (1999). Investigation of Ultrafine Particle Formation during Diesel Exhaust Dilution. *Environ. Sci. Technol.* 33: 3730–3736.

Shi, J.P., Khan, A.A. and Harrison, R.M. (1999). Measurements of Ultrafine Particle Concentration and Size Distribution in the Urban Atmosphere. *Sci. Total Environ.* 235: 51–64.

Silva, L.F.O., Moreno, T. and Querol, X. (2009). An Introductory TEM Study of Fe-nanominerals within Coal Fly Ash. *Sci. Total Environ*. 407: 4972–4974.

Silva, L.F.O., Querol, X., da Boit, K.M., Fdez-Ortiz de, Vallejuelo S. and Madariaga, J.M. (2011). Brazilian Coal Mining Residues and Sulphide Oxidation by Fenton s Reaction: An Accelerated Weathering Procedure to Evaluate Possible Environmental Impact. *J. Hazard. Mater.* 186: 516–525.

Silva, L.F.O., Sampaio, C.H., Guedes, A., Fdez-Ortiz de Vallejuelo, S. and Madariaga, J.M. (2012). Multianalytical Approaches to the Characterisation of Minerals Associated with Coals and the Diagnosis of Their Potential Risk by Using Combined Instrumental Microspectroscopic Techniques and Thermodynamic Speciation. *Fuel* 94: 52–63.

Slezakova, K., Pereira, M.C., Reis, M.A. and Alvim-Ferraz, M.C. (2007). Influence of Traffic Emissions on the Composition of Atmospheric Particles of Different Sizes – Part 1: Concentrations and Elemental Characterization. *J. Atmos. Chem.* 58: 55–68.

Ströher, G.L., Poppi, N.R., Raposo, J.L. and Gomes de Souza, J.B. (2007). Determination of Polycyclic Aromatic Hydrocarbons by Gas Chromatography - Ion Trap Tandem Mass Spectrometry and Source Identifications by Methods of Diagnostic Ratio in the Ambient Air of Campo Grande, Brazil. *Microchem J.* 86: 112–118.

Szczepanski, J. and Vala, M. (1993). Infrared Frequencies and Intensities for Astrophysically Important Polycyclic Aromatic Hydrocarbon Cation. *Astrophys. J.* 414: 646–655.

Teixeira, E.C., Agudelo-Castañeda, D.M., Fachel, J.M.G., Leal, K.A., Garcia, K.D.O. and Wiegand, F. (2012). Source Identification and Seasonal Variation of Polycyclic Aromatic Hydrocarbons Associated with Atmospheric Fine and Coarse Particles in the Metropolitan Area of Porto Alegre, RS, Brazil. *Atmos. Res.* 118: 390–403.

Teixeira, E.C., Mattiuzi, C.D., Agudelo-Castañeda, D.M., Garcia K.O. and Wiegand, F. (2013). Polycyclic Aromatic Hydrocarbons Study in Atmospheric Fine and Coarse Particles Using Diagnostic Ratios and Receptor Model in Urban/Industrial Region. *Environ. Monit. Assess.* 185: 9587–9602.

Tsai, Y. and Kuo, S. (2006). Development of Diffuse Reflectance Infrared Fourier Transform Spectroscopy for the Rapid Characterization of Aerosols. *Atmos. Environ.* 40: 1781–1793.

Tsapakis, M., Lagoudaki, E., Stephanou, E.G., Kavouras, I.G., Koutrakis, P., Oyola, P. and Von Baer, D. (2002). The Composition and Sources of HV $PM_{2.5}$ Organic Aerosol in Two Urban Areas of Chile. *Atmos. Environ.* 36: 3851–3863.

Wang, Y., Szczepanski, J. and Vala, M. (2007). Vibrational Spectroscopy of Neutral Complexes of Fe and Polycyclic Aromatic Hydrocarbons. *Chem. Phys.* 342: 107–118.

Yu, J., Flagan, R.C. and Seinfeld, J.H. (1998). Identification of Products Containing –COOH, -OH, AND –C=O in Atmospheric Oxidation of Hydrocarbons. *Environ. Sci. Technol.* 32: 2357–2370.

Received for review, December 18, 2014
Revised, February 20, 2015
Accepted, March 28, 2015